# RasGEF-containing proteins GbpC and GbpD have differential effects on cell polarity and chemotaxis in *Dictyostelium*

**Leonard Bosgraaf[1], Arjen Waijer[1], Ruchira Engel[2], Antonie J. W. G. Visser[2], Deborah Wessels[3], David Soll[3] and Peter J. M. van Haastert[1,*]**

[1]Department of Biochemistry, University of Groningen, Nijenborgh 4, 9747 AG Groningen, The Netherlands
[2]MicroSpectroscopy Centre, Laboratory of Biochemistry, Wageningen University, Dreijenlaan 3, 6703 HA Wageningen, The Netherlands
[3]W. M. Keck Dynamic Image Analysis Facility, Department of Biological Sciences, University of Iowa, Iowa City, IA 52242, USA
*Author for correspondence (e-mail: haastert@chem.rug.nl)

*Accepted 10 February 2005*
*Journal of Cell Science 118, 1899-1910 Published by The Company of Biologists 2005*
*doi:10.1242/jcs.02317*

## Summary

**The regulation of cell polarity plays an important role in chemotaxis. Previously, two proteins termed GbpC and GbpD were identified in *Dictyostelium*, which contain RasGEF and cyclic nucleotide binding domains. Here we show that *gbpC*-null cells display strongly reduced chemotaxis, because they are unable to polarise effectively in a chemotactic gradient. However, *gbpD*-null mutants exhibit the opposite phenotype: cells display improved chemotaxis and appear hyperpolar, because cells make very few lateral pseudopodia, whereas the leading edge is continuously remodelled. Overexpression of GbpD protein results in severely reduced chemotaxis. Cells extend many bifurcated and lateral pseudopodia, resulting in the absence of a leading edge. Furthermore, cells are flat and adhesive owing to an increased number of substrate-attached pseudopodia. This GbpD phenotype is not dependent on intracellular cGMP or cAMP, like its mammalian homolog PDZ-GEF. Previously we showed that GbpC is a high-affinity cGMP-binding protein that acts via myosin II. We conclude that cGMP activates GbpC, mediating the chemoattractant-induced establishment of cell polarity through myosin. GbpD induces the formation of substrate-attached pseudopodia, resulting in increased attachment and suppression of polarity.**

Key words: Chemotaxis, Polarity, cGMP, PDZ-GEF

## Introduction

*Dictyostelium discoideum* live as unicellular amoebae that feed on bacteria in the soil. Upon starvation, cells start to secrete cAMP that serves as a chemoattractant. After aggregation is complete, a multicellular slug is formed that eventually develops into a fruiting body composed of dead stalk cells and a slime droplet containing viable spores. When *Dictyostelium* cells are placed in a chemoattractant gradient, they become polarised and start to move in the direction of the gradient. Polarisation improves the chemotactic efficiency of the cells and many mutants that have a chemotaxis defect also display a decreased ability to maintain polarity (Bosgraaf et al., 2002a; Khurana et al., 2002; Wessels et al., 1988; Zhang et al., 2003). However, mutant cells that make fewer lateral pseudopodia and consequently appear hyperpolar also aggregate less efficiently compared to the wild type (Zhang et al., 2002). This indicates that a balance exists between the spatial confinement of events leading to polarisation on one hand, and the tendency to make lateral protrusions that allows direction changes on the other.

Actin and conventional myosin (myosin II) play an important role in the cytoskeletal rearrangements that underlie chemotactic movement. In particular, actin polymerisation is crucial for the formation of new protrusions whereas myosin II plays an important role in the maintenance of cell polarity and retraction of pseudopodia and the uropod (Clow and McNally, 1999; Koehl and McNally, 2002; Laevsky and Knecht, 2003; Wessels et al., 1988). Protruding pseudopodia are major sites of actin polymerisation and branching (Condeelis et al., 1988). This is probably mediated by the Arp2/3 complex and by a number of small GTPases (reviewed by Lee et al., 2001).

In contrast to actin, myosin II is mainly localised at the cortex of the posterior half in translocating cells and in retracting pseudopodia (Moores et al., 1996). Studies on myosin heavy chain knockout cells have revealed that myosin is required for cortical tension, efficient chemotaxis and cell polarisation (Egelhoff et al., 1996; Wessels et al., 1988). Myosin is regulated primarily by phosphorylation of the regulatory light chain (RLC) and of the heavy chain (MHC). Phosphorylation of the RLC increases the ATPase activity of myosin II (Griffith et al., 1987), whereas MHC phosphorylation regulates the formation of myosin filaments (Egelhoff et al., 1993; Stites et al., 1998). Chemoattractant stimulation not only leads to the transient phosphorylation of RLC and MHC (Berlot et al., 1985), but also induces the translocation of myosin filaments to the cortex (Liu and Newell, 1991). Recently it was found that the translocation event requires the presence of F-actin (Levi et al., 2002). Furthermore, another recent study indicates that actin polymerisation depends on the phosphorylation state of myosin

(Heid et al., 2004). These findings indicate that actin and myosin cooperate in an intricate signal transduction pathway that is poorly understood.

A number of studies have implicated cGMP as an important mediator of myosin II signalling (reviewed by van Haastert and Kuwayama, 1997). Recently, we identified two guanylyl cyclases and four putative cGMP binding proteins in *Dictyostelium* (Roelofs et al., 2001a; Roelofs et al., 2001b; Goldberg et al., 2002). Two of the cyclic nucleotide binding proteins (GbpA and GbpB) encode non-canonical phosphodiesterases (Bosgraaf et al., 2002a; Bosgraaf et al., 2002b; Meima et al., 2002). The other two proteins (GbpC and GbpD) are presumably the main targets of cGMP, as no other potential cGMP binding candidates could be identified in the nearly completed genome database (http://www.dictybase.org/). GbpC is the high affinity cGMP binding component in *Dictyostelium*, as disruption of the gene caused the loss of all high affinity cGMP binding capacity of cell lysates (Bosgraaf et al., 2002a). GbpC has a unique domain topology and contains small GTPase, kinase, RasGEF, GRAM and two cyclic nucleotide binding domains, respectively. GbpD is homologous to the C-terminal half of GbpC and also contains RasGEF, GRAM and two cyclic nucleotide binding domains. Mutants in which both *gbpC* and *gbpD* are disrupted display severely impaired chemotaxis, which is caused in part by the strongly diminished myosin II translocation to the cortex that was observed in this mutant (Bosgraaf et al., 2002a). Furthermore, MHC phosphorylation and especially RLC phosphorylation was also reduced in *gbpC*$^{-}$/*gbpD*$^{-}$ cells. The same aberrancies were found in a mutant that is unable to produce cGMP owing to the disruption of two guanylyl cyclases (Bosgraaf et al., 2002a). This indicates that a cGMP-mediated pathway acts through GbpC and/or GbpD, leading to the phosphorylation and translocation of myosin II.

Here we report the effect of separate disruption of the *gbpC* and the *gbpD* genes. The results show that the phenotype of *gbpC*$^{-}$ cells is essentially identical to the previously described phenotype of the double *gbpC*$^{-}$/*gbpD*$^{-}$ mutant, both exhibiting a cGMP-dependent, myosin-mediated defect in the suppression of lateral pseudopodia and reduced chemotaxis. Disruption of *gbpD* leads to highly polar elongated cells that exhibit enhanced cell speed, which is accompanied by a decreased substrate adhesion. Furthermore, cells overexpressing GbpD extend many substrate-attached pseudopodia and are impaired in chemotaxis. This phenotype is similar to that of cells overexpressing Rap1 (Rebstein et al., 1993), which may well be a target of GbpD. These data indicate that GbpD induces the formation of substrate-attached pseudopodia that leads to increased adhesion and a concomitant decrease in polarity. Thus, GbpC and GbpD independently affect chemotactic motility in opposing manners.

## Materials and Methods

### Strain and culture conditions

DH1 (a uracil auxotroph wild-type *Dictyostelium*), *gca*$^{-}$/*sgc*$^{-}$ (a guanylyl cyclase-null cell line) (Roelofs and Van Haastert, 2002), and the mutant cell lines described below were grown on HG5 medium (14.3 g/l pepton, 7.15 g/l yeast extract, 10 g/l glucose, 1.36 g/l $Na_2HPO_4.12H_2O$ and 0.49 g/l $KH_2PO_4$) unless indicated otherwise. To select for transformants with one of the extrachromosomal plasmids described below, HG5 was supplemented with 10 μg/ml Geneticin (Gibco) and/or Hygromycin B (Invitrogen).

The *gbpC* or *gbpD* gene was disrupted using gene-specific plasmids that were previously used to make the double *gbpC/gbpD* deletion mutant (Bosgraaf et al., 2002a). Potential knockouts of *gbpC* or *gbpD* were screened by PCR and confirmed by Southern blot analysis.

### Construction of overexpression plasmids

The *gbpD* gene was cloned in five parts by PCR using the Expand Long Template kit (Roche). Each PCR fragment was first separately cloned in pGemTeasy (Promega) and sequenced. The PCR fragments were joined by making use of the restriction sites that are underlined in the primers below. The 5′ part of the gene that encodes the rasGEF domain contains introns and was obtained using reverse-transcriptase PCR with AX3 RNA as a template. Two PCR fragments were obtained with the primer pairs 5′-T**GGATCC**GAAAAAATGACA-GATTACCCATTC-3′ (*Bam*HI site bold) and 5′-GTTATCTAGA-CATCGATGATCTACTTGGA-3′; and 5′-TGGATCCAAAAATG-CATCGATGAAAATGGGTAAAG-3′ with 5′-GTTATCTAGACT-GCAGTGGATGATGATGTCTCTTCTCTAATC-3′. The C-terminal half of the protein was obtained using three PCR fragments with AX3 genomic DNA as a template using the primer pairs: 5′-TGGA-TCCAAAAATGCTGCAGTCATTAAAAGAATCAAATGG-3′ with 5′-GTTATCTAGATTCGAACTACCACCACCATTGCC-3′; 5′-TG-GATCCAAAAATGAGTTCGAATGGTGCGGGTGGTGG-3′ with 5′-TGCTAGCACTAACTGATTGTTGTA-3′; and 5′-TGCTAGCT-CAACAACACCACCTGTAC-3′ with 5′-G**TCTAGA**TTAAGT-TAAATTACGGACAC-3′ (*Xba*I site bold). Finally, the complete *gbpD* gene was released with *Bam*HI and *Xba*I, and cloned between the actin 15 promoter and the actin 8 terminator of MB74 using its *Bgl*II and *Spe*I sites. MB74 is an extrachromosomal shuttle plasmid for *Dictyostelium* derived from MB12NEO (Linskens et al., 1999). Approximately 1-4 μg plasmid was electroporated to the cells as described above.

To fuse the C-terminal part of GbpD with GFP, the same six primers were used as mentioned above, except that the primer 5′-GTTA**TC-TAGA**AGTTAAATTACGGACACGT-3′ (*Xba*I site bold) was used as the reverse primer fragment at the 3′ end of the gene to omit the stop codon. The truncated gene was released using the *Bam*HI and *Xba*I sites and ligated into the *Bgl*II and *Spe*I sites of MB74GFP. The MB74GFP plasmid is similar to MB74 but contains the S65T GFP gene behind the *Spe*I site. The final fusion protein consists of a methionine followed by amino acids 585 to 1312 of GbpD, two serines and the complete S65T GFP protein.

For the fusion of the C-terminal part of GbpC with GFP, two PCR products were obtained using genomic AX3 DNA as a template with the primer pairs 5′-G**AGATCT**AAAAATGACCTCGAGTAATTTC-TTTGGTAATGGTTC-3′ (*Bgl*II site bold) with 5′-GTTATCTA-GAAGTCGACGTTTGAGTACGACCTAAATAAG-3′; and 5′-GAG-ATCTAAAAATGACGTCGACTTCACCATTGAATGAAGG-3′ with 5′-G**TCTAGA**AGCATAAAGTTGTGATTCTCT-3′ (*Xba*I site bold). The fragments were assembled in MB74GFP. The final protein consists of a methionine followed by amino acids 2005 to 2631 of GbpC, two serines and the complete S65T GFP protein.

LimEΔcoil-GFP was made to detect filamentous actin. This was accomplished by amplification of the fragment encoding the first 145 amino acids of LimE using the primers 5′-AA**AGATCT**AAAAAAT-GTCTGCTTCAGTTAAATG-3′ (*Bgl*II site bold) and 5′-TT**ACTAG-T**ACCAGTTGGTTGACCATC-3′ (*Spe*I site bold) using Reverse transcriptase PCR with AX3 RNA as a template. The fragment was ligated in a modified MB74GFP vector that contained a hygromycin- instead of neomycin-resistance cassette. The hygromycin resistance cassette (kind gift of J. Williams, School of Life Sciences, Wellcome Trust Biocentre, University of Dundee, UK) is comprised of an actin 15 promoter followed by the HPH hygromycin resistance gene and the cabA terminator 5′-TAAATAAAATAAATAAATTGT-3′. The final

LimEΔcoil-GFP fusion protein consists of amino acids 1 to 145 of LimE, a threonine and serine residue and the complete S65T GFP protein.

### cAMP-induced myosin-GFP translocation

The myosin heavy chain-GFP overexpressor construct was a kind gift from T. Egelhoff. Cells expressing this construct were starved in six-well plates (Nunc) under 2 ml PB (10 mM Na/K phosphate, pH 6.5) until the onset of aggregation. Cells were washed off and transferred to a custom-made flow chamber that has been described previously (Potma et al., 2001). After adherence for 10 minutes, cells were stimulated with $10^{-6}$ M cAMP. Confocal images were taken every 5 seconds with a confocal laser-scanning microscope (Zeiss ConfoCor 2-LSM 510 combination set up). Images were analysed with the QuimP software package version 1 (http://www.garching-innovation.de/e_akterf/e_softwa/e_softtxt/quimp/QuimP-guide/) (Dormann et al., 2002).

### Actin polymerisation assay

Actin polymerisation assay was carried out as described (Zigmond et al., 1997). Briefly, 5-hour starved and pulsed cells were incubated in PM (2 mM $MgCl_2$ in 10 mM Na/K phosphate, pH 6.5) with 2 mM caffeine at $3\times10^7$ cells/ml. After 20 minutes, 1.1 ml cell suspension was stimulated at $t$=0 with 200 nM cAMP. At the indicated time points, 100 μl samples were taken and transferred to 1 ml AB (20 mM $KPO_4$, 10 mM PIPES, 5 mM EGTA, 2 mM $MgCl_2$, 3.7% formaldehyde, 0.1% Triton X-100, 0.25 μM TRITC-Phalloidin, pH 6.8). After shaking for 1 hour at room temperature, samples were centrifuged for 10 minutes at 14,000 ***g*** and the resulting pellet was resuspended in 1 ml methanol. After shaking overnight, the amount of F-actin was determined by measuring the fluorescence (excitation 540 nm, emission 565 nm).

### Adhesion assay

To quantify the strength of cell adhesion to the surface, we used a previously published protocol (Fey et al., 2002) with a few modifications. Cells were grown on HG5 in six-well plates from Nunc to maximum 60% confluency. The medium was replaced by 2 ml PB and the plates were incubated for 1 hour. Then, the plates were rotated on a rotary shaker at 150 rpm and 150 μl samples were taken at the indicated time points. The wells were replenished with fresh PB. After the final time point, the remaining cells were detached thoroughly by repeated pipetting. After vortexing for 15 seconds, the number of cells in the samples was determined in quadruple using a haemocytometer. The number of cells removed at previous time points was added to the amount of loose cells and divided by the total number of cells on the plate to yield the percentage of loose cells.

### Determination of intracellular cAMP and cGMP concentrations

To determine the amount of intracellular cAMP and cGMP, $5\times10^8$ cells were washed once with 50 ml PB and centrifuged at 450 ***g*** for 3 minutes. The cell pellet was resuspended in PB to a volume of 400 μl and an equal volume of 3.5% (v/v) perchloric acid was added. The samples were centrifuged for 5 minutes at 14,000 ***g***, the supernatant was neutralised with 200 μl $KHCO_3$ (50% saturated solution), centrifuged again for 5 minutes at 14,000 ***g***, and the supernatant was collected. The amount of cAMP and cGMP was determined using the cAMP and cGMP assay systems from Amersham. The assays contained 50 μl supernatant derived from $2.5\times10^7$ cells. In the absence of cAMP or cGMP the assays yield 0±0.0097 pmol cAMP/assay and 0±0.0076 pmol cGMP/assay, respectively ($n$=6). This implies that the sensitivity of the assay is 0.024 pmol cAMP/$10^7$ cells and 0.019 pmol cGMP/$10^7$ cells. The data obtained for the cell extracts are in pmol/$10^7$ cells ($n$=4): wild type, 0.20±0.05 cAMP and 0.89±0.19 cGMP; *gbpD*$^-$/GbpD$^{OE}$, 0.23±0.03 cAMP and 0.89±0.10 cGMP; *gbpD*$^-$/GbpB$^{OE}$/GbpD$^{OE}$, 0.004±0.031 cAMP and 1.01±0.09 cGMP; *gca*$^-$/*sgc*$^-$/GbpD$^{OE}$, 0.18±0.02 cAMP and 0.03±0.05 cGMP; *gca*$^-$/*sgc*$^-$/GbpB$^{OE}$/GbpD$^{OE}$, –0.004±0.016 cAMP and –0.01±0.04 cGMP. The data show that guanylyl cyclase-null cells have normal cAMP levels, but no detectable cGMP (detection limit 0.19 pmol/$10^7$ cells), whereas cells overexpressing GbpB have normal cGMP levels and no detectable cAMP (detection limit 0.024 pmol/$10^7$ cells).

### Computer-assisted analysis of single cell chemotaxis in a spatial gradient of cAMP

To initiate development, growth phase cells were washed in buffered salts solution (BSS) containing 20 mM KCl, 2.5 mM $MgCl_2$ and 20 mM $KH_2PO_4$ (pH 6.4), and dispersed on a black filter pad saturated with BSS at a density of $5\times10^6$ cells per $cm^2$. Amoebae were washed off the filter pads at the ripple stage, which in dense cultures represents the onset of aggregation, the time at which *Dictyostelium* amoebae attain their highest average velocity (Varnum and Soll, 1984). In this case, the onset of aggregation was observed between 8 and 11 hours, depending on the particular strain.

The motile behaviour of cells in buffer and in spatial gradients of cAMP was analysed using computer-assisted methods previously described (Soll, 1995; Soll et al., 2001). Briefly, cells were dispersed on the bridge of a Plexiglas gradient chamber, in which one of the two troughs bordering the bridge contained BSS and the other trough contained BSS plus $10^{-6}$ M cAMP. Cells were video recorded through a 25× objective with bright field optics for a 10 minute period following an initial 5 minute incubation period necessary for establishing a steep gradient of cAMP. Images were digitised at a rate of 15 frames per minute. 2D-DIAS software then automatically outlined the cell perimeters and converted them to beta-spline replacement images from which the position of the cell centroid was determined. Chemotactic index, speed and change of direction were computed from the centroid position as described (Soll, 1995; Soll et al., 2001).

### cGMP and cAMP binding assay

Cells were starved for 1 hour in starvation buffer (40 mM HEPES/NaOH, pH 7.0), washed and resuspended at a density of $2\times10^8$ cells/ml in starvation buffer supplemented with 0.25 M sucrose, 0.5 mM EDTA, 0.5 mM EGTA and one protease inhibitor cocktail tablet (mini Complete-tablets, EDTA-free from Roche) per 10 ml buffer. Cells were immediately lysed by passage through a 0.45 μm Nuclepore filter. The lysate was centrifuged for 2 minutes at 14,000 ***g*** and the supernatant was centrifuged again for 4 minutes at 14,000 ***g***. 100 μl of the newly obtained supernatant was added to 100 μl assay buffer containing 40 mM HEPES/NaOH pH 7.0, 0.5 mM EGTA, 6 mM $MgCl_2$, 10 mM dithiothreitol, 10nM 8-Br-cAMP, 100 nM [$^3$H]cGMP. This mixture was incubated on ice for 20 minutes followed by filtration of the mixture over nitrocellulose filters (pore size 0.45 μm) and the filters were washed twice with 3 ml ice-cold 40 mM HEPES/NaOH pH 7.0. After drying, 3 ml scintillation liquid was added and the radioactivity associated with the filters was determined using a liquid scintillation counter. To determine non-specific binding 500 μM cGMP was included in the assay mixture. For measurement of the binding of 5 nM [$^3$H]cGMP (Fig. 6B), the same procedure was applied, with a few modifications: the precleared lysate was centrifuged for 60 minutes at 48,000 ***g***; assay buffer contained 100 mM PB, 10 mM dithiothreitol, 6 mM $MgCl_2$ and 5 nM [$^3$H]cGMP; 5 μM unlabelled cGMP was used to determine non-specific binding and 50 mM PB was used to wash the filters.

**Table 1. Chemotactic behaviour of mutant cells in a spatial gradient of cAMP**

| Cell line | Wild type (DH1) | *gbpC*$^{-}$ | *gbpC*$^{-}$/*gbpD*$^{-}$ | *gbpD*$^{-}$ | *gbpD*$^{-}$/GbpD$^{OE}$ |
|---|---|---|---|---|---|
| Number of cells | 32 | 37 | 59 | 54 | 36 |
| Chemotaxis index | 0.44±0.30 | 0.08±0.16** | 0.05±0.12** | 0.58±0.25* | 0.06±0.33** |
| Speed (μm/minute) | 9.1±4.7 | 3.4±1.2** | 3.5±1.4** | 20.5±8.3** | 5.4±4.1* |
| Direction change (degrees/minute) | 24±9 | 53±16** | 53±13** | 27±11 NS | 40±13** |
| Roundness (%) | 64±15 | 81±10** | 77±11** | 44±9** | 49±9** |
| Lateral pseudopod (/10 minutes)[†] | 1.33±1.48 | ND | ND | 0.46±0.98* | 5.52±2.56** |
| Pseudopod bifurcation (/10 minutes)[‡] | 4.88±4.14 | ND | ND | 1.76±2.58* | 13.93±4.97** |

Values are means±s.d. Values significantly different from levels in the wild type are indicated as *$P$<0.05 and **$P$<0.001. NS, not significantly different from levels in the wild type at $P$>0.05. ND, not determined; owing to the low speed and high roundness of the *gbpC*$^{-}$ and *gbpC*$^{-}$/*gbpD*$^{-}$ mutants, the frequency of pseudopod bifurcation and lateral pseudopod formation could not be determined reliably.

[†]A lateral pseudopod was considered to be a projection formed from the main axis of translocation at an angle ≥30° that attained a minimum of 5% total cell area and emanated from the posterior two-thirds of the cell. The main axis of translocation was determined by drawing a line between the centroid of the cell in the frame 15 seconds earlier and the centroid of the cell in the present frame.

[‡]Pseudopod bifurcation was considered to be a projection formed from the main axis of translocation at an angle ≥30° that attained a minimum of 5% total cell area and emanated from the anterior one-third of the cell.

## Results

### Altered chemotaxis of Gbp mutants

To study the role of GbpC and GbpD, we have created cell lines in which either the *gbpC* or *gbpD* gene is disrupted. This was accomplished by homologous recombination in the *Dictyostelium* uracil auxotroph DH1, using pyr5/6 as a selection marker for *gbpD* and Bsr for *gbpC*. A double knockout was obtained by inactivating the *gbpC* gene in the *gbpD* knockout, as described (Bosgraaf et al., 2002a). All knockout cells grew with a normal rate in axenic medium and on bacterial lawns, and developed normally, although *gbpC*$^{-}$ mutant cells made somewhat smaller fruiting bodies (data not shown).

We subjected starved *gbpC*$^{-}$ and *gbpD*$^{-}$ single knockout cells to a chemotaxis analysis using the DIAS software package. When placed in a spatial gradient of cAMP, *gbpC*$^{-}$ cells failed to become elongated and moved much more slowly and less persistently than wild-type cells (see Table 1 and Fig. 1A). Moreover, the chemotaxis index, which is defined as the movement towards the cAMP source divided by the total cell movement, was greatly diminished. The polarity of a cell is reflected in the parameter 'roundness'; a perfect circle would have a roundness of 100 whereas a straight line would have a roundness of 1. As reported in Table 1, *gbpC*$^{-}$ cells were significantly rounder than wild-type cells. These characteristics closely resemble the phenotype of the *gbpC*$^{-}$/*gbpD*$^{-}$ cells that was described before (Bosgraaf et al., 2002a).

As opposed to the *gbpC*$^{-}$ and *gbpC*$^{-}$/*gbpD*$^{-}$ double knockout cells, *gbpD*$^{-}$ cells appeared very polar and moved with increased speed and efficiency towards the cAMP source (see Table 1 and Fig. 1A). The increased polarity is reflected in a decreased roundness. It was also observed that the *gbpD*$^{-}$ cells often wiggled for a while with only the uropod attached to the substratum. This was accompanied by a looser adherence to the substratum of *gbpD*$^{-}$ cells in general (see below). In fact, the decreased substrate adhesion is presumably the primary cause of the increased cell speed and chemotaxis performance. Although the tracks of some *gbpD*$^{-}$ cells undergoing chemotaxis suggest that the cells might turn by making lateral pseudopodia or bifurcation of the anterior pseudopod, separate images of the cells taken at different time points clearly indicate that the cells almost never made lateral protrusions (Fig. 1B). Rather, the cells turned by making a new anterior pseudopodium to a slightly different direction. Indeed, as shown in Table 1, *gbpD*$^{-}$ cells made on average 0.46 lateral pseudopodia per 10 minutes, a significant decrease compared to wild-type cells that made 1.33 lateral pseudopodia in 10 minutes. Furthermore, the frequency of anterior pseudopod bifurcation, which often leads to a direction change, was lowered in *gbpD*$^{-}$ cells (1.76 per 10 minutes) when compared to wild-type cells in which 4.88 pseudopodia bifurcated per 10 minutes (Table 1). These findings indicate that *gbpD*$^{-}$ cells displayed enhanced chemotaxis due to an increased integrity of the leading pseudopod and a reduced tendency to produce lateral pseudopodia.

In order to rescue the phenotype of the *gbpD*$^{-}$ mutants, the *gbpD* gene was overexpressed using an extrachromosomal expression plasmid. Surprisingly, the resulting *gbpD*$^{-}$/GbpD$^{OE}$ cells were large, flattened and contained many filopodial protrusions and lamellipodia at the substrate surface (described in detail below). Furthermore, this mutant attached more strongly to the surface than wild-type cells (see below). The *gbpD*$^{-}$/GbpD$^{OE}$ cells were unable to aggregate and this could not be rescued by synergistic development with wild-type cells (not shown). The *gbpD*$^{-}$/GbpD$^{OE}$ cells displayed very poor chemotaxis when subjected to a cAMP gradient (Fig. 1A, Table 1). The cells produced many pseudopodia that were often bifurcated or filopod-like. Nevertheless, the cells were able to move directionally, albeit with decreased speed. The reduction of cell speed is probably caused by the increased substrate adhesion and the greater number of pseudopodia produced. Although the cells were able to move persistently, the direction of movement was almost random, an observation that was confirmed by the calculated chemotaxis index that was only 0.06 for this mutant. This lack of chemotaxis was presumably caused by the large amount of lateral pseudopodia that the cells formed (four times more than seen in the wild type) and the extreme extent of pseudopod bifurcation (three times more than that in the wild type), which hindered the formation of a dominant anterior pseudopod (Table 1). We observed that about 10% of the cells had a much higher speed and displayed clear positive chemotaxis. As expression levels of ectopic genes are generally very heterogeneous in *Dictyostelium*, we believe that these cells had very low expression levels of *gbpD*.

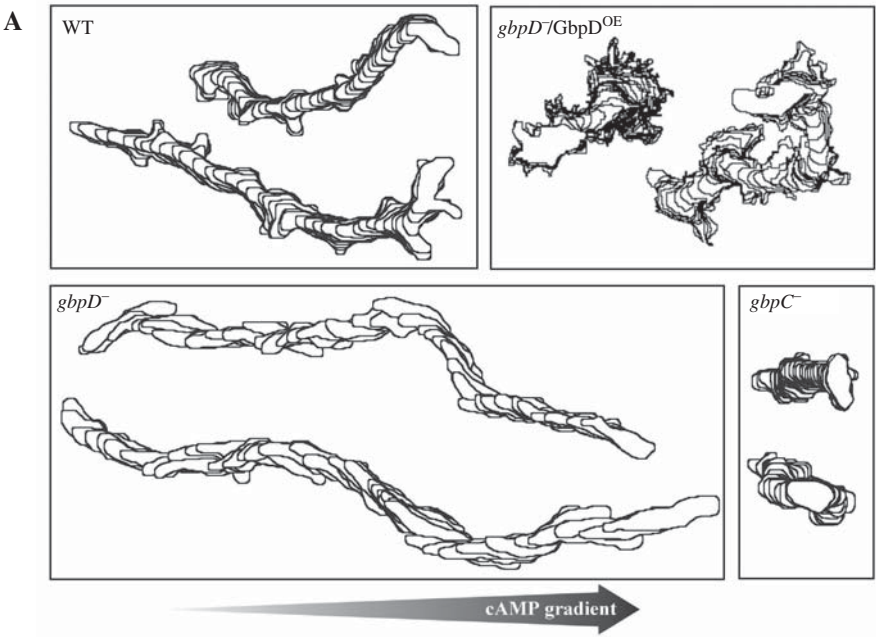


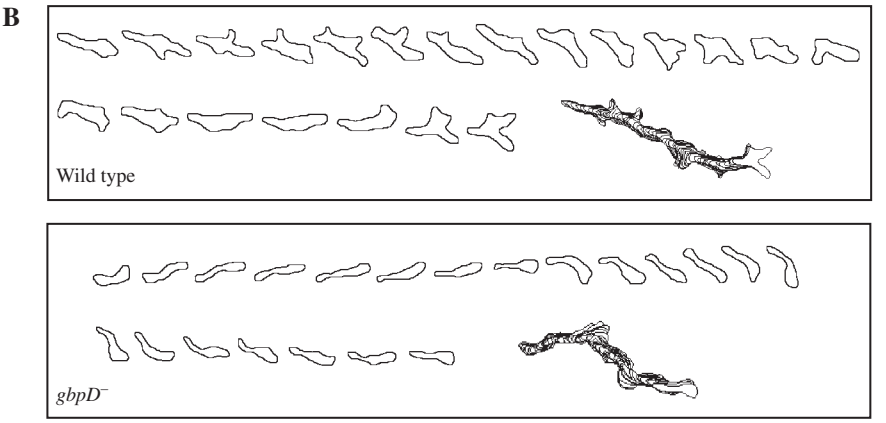


**Fig. 1.** Chemotaxis of *gbpC* and *gbpD* mutants. (A) Cell tracks of representative wild-type (WT) and mutant *Dictyostelium* cells in a spatial gradient of cAMP. Cells were starved until the ripple stage was reached. Subsequently, they were placed in a chemotaxis chamber filled with phosphate buffer at one end and phosphate buffer with cAMP at the other end. Images were taken every 10 seconds for a period of 5 minutes and the cell outlines of subsequent images were placed on top of each other to obtain the final picture. (B) Cell tracks and separate images of a wild-type and a *gbpD*⁻ cell that were placed in a chemotaxis chamber. The tracks are composed of stacked images that were taken every 4 seconds. Every third frame is also shown as a separate image.

When these cells were excluded from the chemotaxis analysis, the chemotaxis index dropped to –0.01 and the percentage of cells that moved in the direction of the gradient was only 55%, very close to random movement, which would result in 50% of the cells moving towards the chemoattractant and 50% away. These data illustrate that overexpression of GbpD caused a near total loss of the ability to undergo chemotaxis.

## Increased substrate attachment in GbpD overexpressing cells

As mentioned before, *gbpD*⁻ cells seemed less well attached to the substratum than wild-type cells, whereas *gbpD*⁻/GbpD$^{OE}$ cells appeared very adhesive. Therefore the adhesion capability of these mutants was quantified by shaking petri dishes seeded with cells and counting the number of cells that detached from the substratum at different time points. The *gbpD*⁻ cells detached much faster from the substratum when compared to wild-type cells (Fig. 2), whereas *gbpD*⁻/GbpD$^{OE}$ cells were much more resistant to detachment. These data suggest that GbpD plays a role in attachment of the cells to the substratum.

## Visualisation of F-actin reveals abnormal phenotype of GbpD overexpressing cells

As *gbpD*⁻/GbpD$^{OE}$ cells produced many filopodial extensions, we were interested in the actin distribution in this cell line. To visualise filamentous actin in living cells, the first 145 amino acids of the F-actin binding protein LimE were fused to GFP (LimEΔcoil-GFP). This part of the protein lacks the C-terminal coiled coil domain but retains the ability to bind F-actin (Schneider et al., 2003). When *gbpD*⁻ cells were transformed with this construct, fluorescence was typically enhanced in leading edges of starved cells (Fig. 3). Furthermore, when a confocal image was taken just above the glass surface, F-actin-rich foci could be detected, as described before (Uchida and Yumura, 2004). Thus, the distribution of F-actin appears normal in *gbpD*⁻cells. In contrast, when *gbpD*⁻/GbpD$^{OE}$

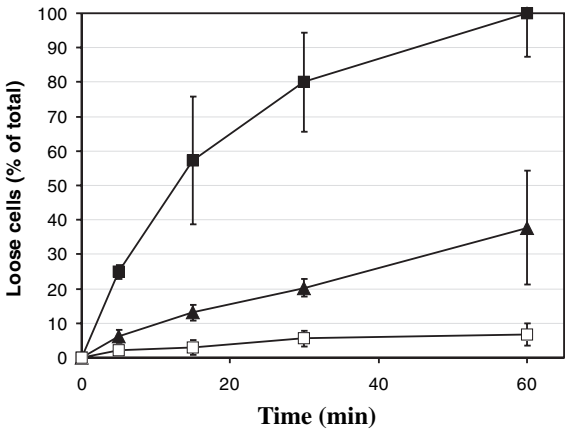


**Fig. 2.** Adhesion strength of vegetative *gbpD*⁻ and GbpD$^{OE}$ cells. The percentage of cells that became detached upon shaking of the culture dish at 150 rpm is plotted against the time of shaking. Symbols indicate the wild type (▲), *gbpD*⁻ (■) and *gbpD*⁻/GbpD $^{OE}$ cells (□). Error bars represent the s.d. of three independent experiments.

mutants were transformed with the same construct, many GFP-labelled protrusions were visible in these cells (Fig. 3). A cross section of a cell revealed that they are more flattened than the parental strain. Measurements of 19 different cells revealed that the contact area is 80% larger than in *gbpD*$^-$ cells whereas the volume has decreased slightly (Table 2). As actin foci transmit force to the substratum (Uchida and Yumura, 2004) and overexpression of GbpD protein caused a much stronger attachment to the substrate, it might be expected that the amount of actin foci would also be higher in *gbpD*$^-$/GbpD$^{OE}$ cells. However, the number of actin foci in *gbpD*$^-$/GbpD$^{OE}$ cells was not significantly higher than in *gbpD*$^-$ cells (Table 2). On the other hand, the number of protrusions that made surface contact was significantly higher in *gbpD*$^-$/GbpD$^{OE}$ cells compared to the parental *gbpD*$^-$ cells. These findings indicate that overexpression of GbpD protein causes an increase in the amount of substrate-attached protrusions, which results in a flattened cell morphology and stronger substrate adhesion.

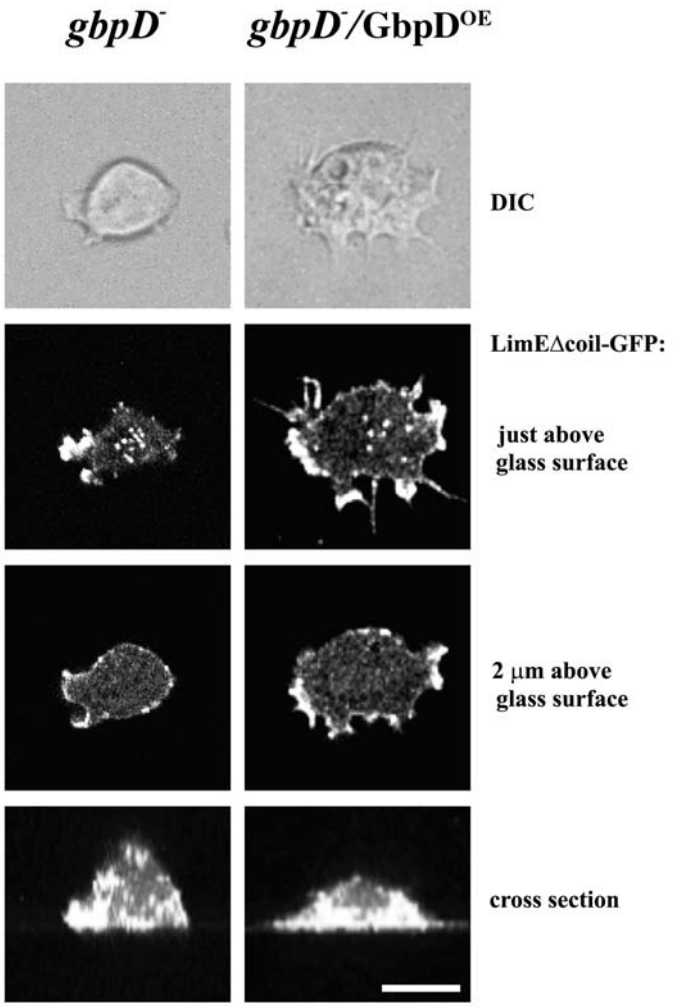


**Fig. 3.** Morphology of *Dictyostelium* cells overexpressing GbpD protein. Confocal images of starved *gbpD*$^-$ and *gbpD*$^-$/GbpD$^{OE}$ cells expressing the F-actin binding domain of LimE fused to GFP. The DIC image and the uppermost fluorescent image were taken just above the glass surface. The second fluorescent image was taken ~2 μm above the glass surface. The thickness of the images corresponds to ~1 μm. The cross section image was obtained by making use of the projection option of the Zeiss LSM Image browser 5 program. White arrowheads indicate the height of the upper two fluorescent images. Bar, 10 μm.

**Table 2. Cell properties of the GbpD overexpressor mutant**

| | *gbpD*$^-$ (*n*=20) | *gbpD*$^-$/GbpD$^{OE}$ (*n*=19) |
|---|---|---|
| Actin foci per cell | 1.84±0.54 | 2.96±0.64 $^{NS}$ |
| Surface-attached protrusions per cell | 2.96±0.26 | 4.87±0.48** |
| Contact area (μm$^2$) | 270±25 | 480±54** |
| Volume (μm$^3$) | 2781±194 | 2082±251* |

Data are derived from the Z-scans of LimEΔcoil-GFP transformed GbpD mutant cells (Fig. 3). Values are means±s.d. Values significantly different to levels in *gbpD*$^-$ cells are indicated as *$P$<0.05 and **$P$<0.01. NS, not significantly different from values in *gbpD*$^-$ cells at $P$>0.05.

## cAMP-induced actin polymerisation in Gbp mutants

The mutants were subjected to a phalloidin binding assay to measure cAMP-induced changes in the amount of filamentous actin. For this experiment, the cells were kept in suspension and pulsed with exogenous cAMP for 4 hours. A typical experiment is shown in Fig. 4. In wild-type cells, a twofold increase in the amount of F-actin was observed that reached its maximum 4-8 seconds after cAMP stimulation, whereas basal levels were recovered after 40-60 seconds. The actin response of both the *gbpD*$^-$ and the *gbpC*$^-$ cells displayed no obvious aberrancies. As the *gbpD*$^-$/GbpD$^{OE}$ cells produce many pseudopodia containing F-actin when attached to a surface, it might be expected that the total F-actin content would be elevated before stimulation in these cells. Surprisingly, we did not observe a significant difference in basal F-actin levels in this or any of the mutants in our experiments (data not shown). However, the *gbpD*$^-$/GbpD$^{OE}$ cells did show a somewhat aberrant F-actin response upon cAMP-stimulation: maximum F-actin levels were lowered to around 70% of that of the wild type. Moreover, pre-stimulus levels were not reached until 90 seconds after stimulation in this mutant, compared to 45

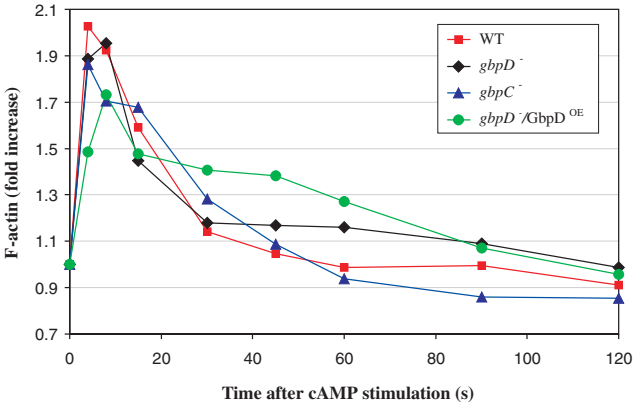


**Fig. 4.** cAMP-induced F-actin formation as measured with a phalloidin binding assay. Aggregation competent wild-type (WT) and mutant cells were stimulated with cAMP and the F-actin content was determined at the indicated time points. The presented values are the average of two independent experiments with error bars indicating standard deviations.

seconds in wild-type cells. We conclude that overexpression of GbpD protein mildly affects the F-actin response, whereas disruption of gbpC or gbpD has no obvious effect on the actin response.

### Altered cAMP-induced myosin II translocation in *gbpC*⁻ mutant

Stimulation with extracellular cAMP is known to induce myosin II translocation to the cortex, a process that depends on intracellular cGMP (Bosgraaf et al., 2002a). Therefore the cAMP-induced myosin II translocation was investigated in *gbpC*⁻ and *gbpD*⁻ cells. This was accomplished by cAMP stimulation of Gbp mutant cells overexpressing GFP-myosin II and taking confocal images at 5-second intervals, as described (Levi et al., 2002). We observed that in wild-type cells, a small but significant portion of the myosin-GFP was present at the cell membrane prior to stimulation (Fig. 5A). This was not overcome by prolonged incubation with caffeine that inhibits the cAMP production of the cells. Within 10 seconds after stimulation with exogenous cAMP, most of this membrane-associated myosin was released into the cytosol (Fig. 5B). This depletion was followed by a rapid and enhanced re-translocation of myosin-GFP to the membrane which was maximal about 30 seconds after stimulation with cAMP. Myosin was subsequently released again from the membrane around 50 seconds after cAMP addition. During the first 60 seconds after cAMP stimulation, cell movement halted. After this period cells started to move again, and myosin-GFP was primarily found in the cytosol and at the membrane in the typical 'C-shape' located at the posterior of the cell (data not shown).

In contrast to wild-type cells, no cAMP-induced myosin II translocation could be detected in *gbpC*⁻ cells during the first 80 seconds after stimulation (Fig. 5B). Instead, a prolonged depletion of myosin-GFP from the membrane was observed, that recovered to pre-stimulus levels after 50 seconds. These data correspond well with our previous finding that cAMP-induced myosin II translocation is abolished in *gbpC*⁻/*gbpD*⁻ cells. The *gbpD*⁻ cells were also transfected with myosin-GFP. When these cells were stimulated with cAMP, myosin-GFP translocation was similar to that observed in wild-type cells (Fig. 5B); myosin-GFP dissociated from the membrane during the first 15 seconds and re-associated with the membrane immediately thereafter for a period of about 45 seconds. Possibly the initial release of myosin II from the membrane is somewhat stronger in the *gbpD*⁻ cell line than in wild-type cells. We

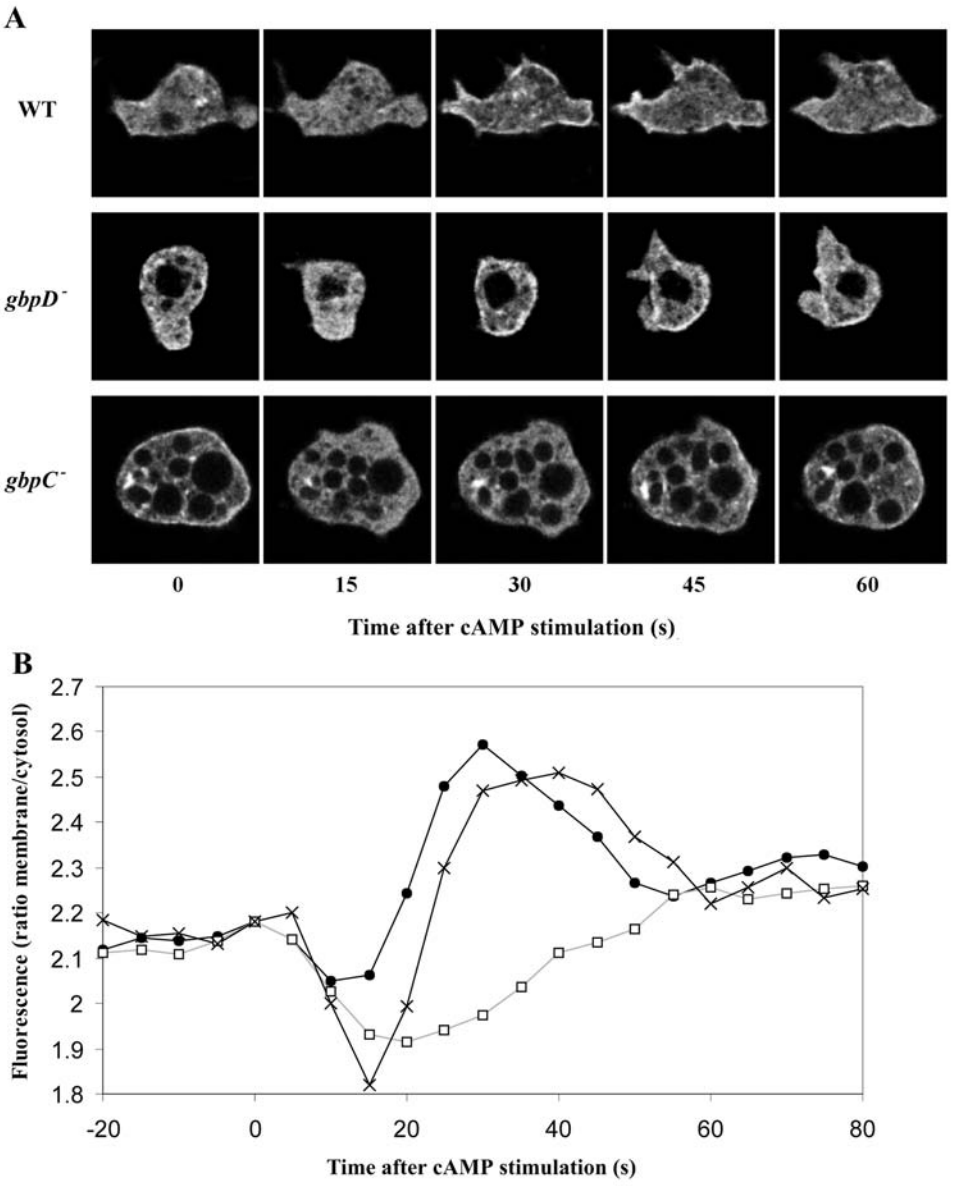


**Fig. 5.** cAMP-induced myosin II translocation. Wild-type cells and mutant cells expressing myosin II-GFP were starved and stimulated with cAMP. (A) Confocal fluorescent images were taken every 5 seconds and are shown at the indicated time points after cAMP stimulation. The *gbpC*⁻ cells contained unusual amounts of vacuoles in this particular experiment. (B) Quantification of the data using the QuimP software developed by T. Bretschneider (Dormann et al., 2002). Fluorescence at the membrane and in the cytosol was calculated and the ratio of the fluorescence at the membrane divided by the average cytosolic fluorescence was plotted against time. In *gbpD*⁻ (×) and wild-type cells (●), myosin translocates to the cortex after an initial depletion. In *gbpC*⁻ cells (□), this myosin translocation to the cortex is absent and depletion of the fluorescent signal from the cortex is prolonged and enhanced. The displayed data are averaged values from 13 wild-type cells, nine *gbpC*⁻ cells and seven *gbpD*⁻ cells from two or three experiments.

conclude that GbpC is necessary for cAMP-induced myosin translocation to the cortex whereas disruption of the *gbpD* gene does not influence this process.

## cGMP and cAMP binding activity in cells overexpressing GbpD protein

GbpD contains a RasGEF domain and two cyclic nucleotide binding domains. These domains are also present in human Epac and PDZ-GEF, but only Epac is stimulated by cAMP whereas the RasGEF activity of PDZ-GEF is not regulated by cAMP or cGMP (de Rooij et al., 1998; Kuiperij et al., 2003; Rehmann et al., 2003). To test whether GbpD is regulated by cyclic nucleotides, the binding properties of this protein were studied by overexpressing GbpD. It has previously been determined that GbpC specifically binds cGMP with an affinity of 4 nM (Bosgraaf et al., 2002a). As such high affinity binding activity obscures the measurement of lower affinity components in cell lysates, the *gbpC*$^{-}$/*gbpD*$^{-}$ mutant was used as a background strain to overexpress GbpD protein. Under the conditions we tested, we could not measure any significant increase in cAMP or cGMP binding activity in the lysates of *gbpC*$^{-}$/*gbpD*$^{-}$/GbpD$^{OE}$ cells when compared to the control cell line (Fig. 6A). We did, however observe a significant decrease in the amount of cAMP binding in cells overexpressing GbpD protein. cAMP binding to lysates of wild-type cells is predominantly to the regulatory subunit of PKA (Mutzel et al., 1988). Therefore, the decreased cAMP binding capacity in lysates of GbpD-overexpressing cells could be caused by a decreased expression of PKA. Because of this, and as overexpression of GbpD protein causes a severe change of cell morphology and behaviour, the C-terminal half of GbpD fused with GFP at its C-terminus was also expressed. This construct, ΔNGbpD-GFP, contains both cyclic nucleotide binding domains but does not contain the rasGEF domain. The corresponding truncated GbpC-GFP fusion protein, which is homologous to GbpD, retains its ability to bind cGMP (Fig. 6B). The ΔNGbpD-GFP fusion protein could be expressed at high levels without affecting the morphology of the cells (data not shown). However, we did not observe any significant increase in cAMP or cGMP binding activity compared to the background strain (Fig. 6A). This result was unaffected by clearing the cell lysate using high-speed centrifugation or changing the assay buffer to phosphate buffer (data not shown). Because the ΔNGbpD-GFP fusion protein was partly localised at the membrane, the membrane fraction of the cell lysates was also investigated for increased cyclic nucleotide binding. Also in this case, the expression of the ΔNGbpD-GFP fusion protein did not result in a measurable increase in cyclic nucleotide binding capacity (data not shown). We also tried to immunopurify the ΔNGbpD-GFP fusion protein using a pull-down assay with GFP antibody. Again, no increase in binding capacity was found in ΔNGbpD-GFP expressing cells compared to control cells (data not shown). Thus, at present we do not have any evidence that GbpD binds either cAMP or cGMP in vitro.

## Adhesion strength of cAMP and cGMP mutants overexpressing GbpD protein

Although we do not have any indication that GbpD binds cyclic nucleotides in vitro, the increased adhesion strength of cells overexpressing GbpD might depend on cyclic nucleotides. To test this, mutants with altered cyclic nucleotide levels were transformed with the GbpD overexpression construct. In the *gca*$^{-}$/*sgc*$^{-}$ cell line, the two known guanylyl cyclases, guanylyl cyclase A and soluble guanylyl cyclase, have been disrupted and these cells no longer have detectable cGMP (see Materials and Methods) (Roelofs and Van Haastert, 2002). When GbpD was overexpressed in this mutant, the same increase in attachment was found as in *gbpD*$^{-}$/GbpD$^{OE}$ cells (Fig. 7). Thus, we conclude that the role of GbpD in attachment of the cells to the substratum is not cGMP dependent. To test whether cAMP is needed for GbpD function, GbpB was overexpressed in the GbpD-overexpressing mutants. GbpB is a very active phosphodiesterase that predominantly hydrolyses cAMP, and it was previously shown that overexpression of this enzyme results in very low cAMP levels (Bosgraaf et al., 2002b). Overexpression of GbpB in *gbpD*$^{-}$/GbpD$^{OE}$ cells led to a very strong decline of the cAMP concentration to undetectable levels (below 0.024 pmol/$10^7$ cells compared to 0.23±0.03 pmol/$10^7$ cells in the parental strain; see Materials and Methods). The adhesion strength of the *gbpD*$^{-}$/GbpD$^{OE}$/GbpB$^{OE}$ mutant was virtually identical to that of *gbpD*$^{-}$/GbpD$^{OE}$ cells as judged by the amount of cells that detached from the surface after shaking the plate for 1 hour (Fig. 7). Thus the GbpD-induced

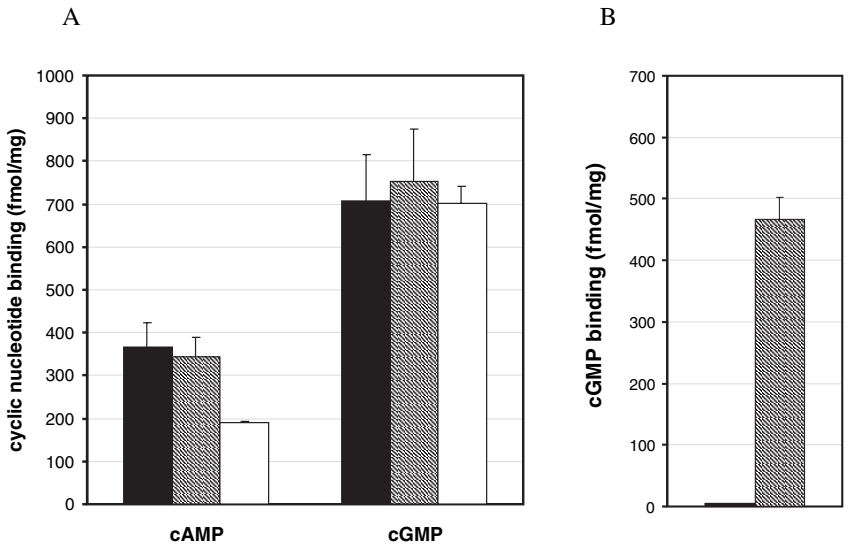


**Fig. 6.** cAMP and cGMP binding to the lysates of mutant cells. (A) Binding of 50 nM [$^3$H]cGMP or [$^3$H]cAMP to the cytosolic fraction of a cell lysate was measured. The results are expressed as the amount of cyclic nucleotide bound per mg protein. The black bar represent lysates of *gbpC*$^{-}$/*gbpD*$^{-}$ cells, the grey bar, *gbpC*$^{-}$/*gbpD*$^{-}$/ΔN-GbpD-GFP$^{OE}$ cells and the white bar, lysates of *gbpC*$^{-}$/*gbpD*$^{-}$/GbpD$^{OE}$ cells. (B) Binding of 5 nM [$^3$H]cGMP to the cytosolic fraction of lysates of *gbpC*$^{-}$ cells (black bar) and *gbpC*$^{-}$/ΔN-GbpC-GFP$^{OE}$ cells (grey bar) was measured. The means±s.d. of at least two independent experiments with quadruple determinations are shown.

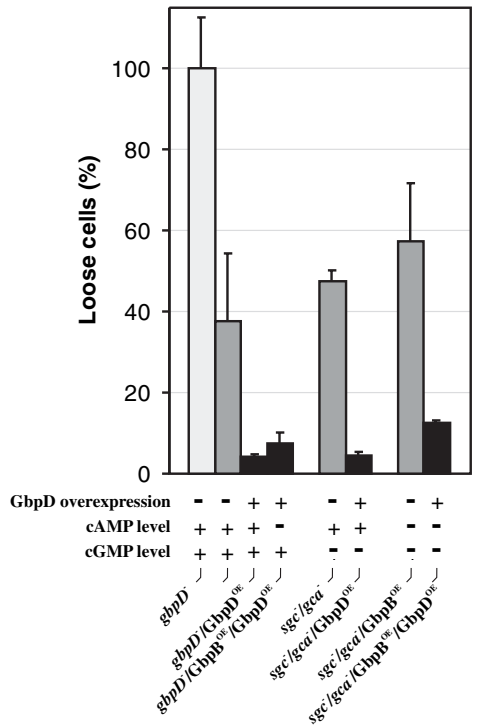


**Fig. 7.** The effect of GbpD overexpression on the adhesion strength of mutants with undetectable cyclic nucleotide levels. The adhesion strength of several mutants was studied by measuring the percentage of cells that became detached from the substrate after shaking for 60 minutes at 150 rpm. The requirement of cGMP for GbpD function was studied by overexpressing GbpD in a guanylyl cyclase double knockout, *sgc*$^{-}$/*gca*$^{-}$; cGMP levels of this cell line were below the detection limit (0.019 pmol/$10^7$ cells or ~3 nM). To study the requirement of cAMP for GbpD function, the phosphodiesterase GbpB was overexpressed. This led to cAMP levels that were below the detection limit of the assay (0.024 pmol/$10^7$ cells or ~4 nM). Finally, GbpD was overexpressed in a cell line that was devoid of cAMP and cGMP by overexpressing GbpB protein in the *sgc*$^{-}$/*gca*$^{-}$ cell line (both cGMP and cAMP levels were below the detection limit). Error bars represent the s.d. of at least two independent experiments.

increase in adhesion strength does not depend on the presence of cAMP either. However, it might be possible that the cyclic nucleotide binding domain(s) of GbpD does not discriminate between cAMP and cGMP. In that case, the presence of either cyclic nucleotide could suffice to activate the protein. Therefore, GbpD was also overexpressed in *gca*$^{-}$/*sgc*$^{-}$/GbpB$^{OE}$ cells, in which the level of either cyclic nucleotide is below the detection limit (see Materials and Methods). In this strain, GbpD overexpression also resulted in dramatically increased adhesion strength, although to slightly lower levels than in wild-type cells (Fig. 7). These findings strongly suggest that GbpD can function in the absence of both cGMP and cAMP, as has been observed for human PDZ-GEF.

## Discussion

### Chemotaxis of Gbp mutants

Deletion of *gbpC* yields cells that display reduced chemotaxis due to slower movement and reduced polarity. This phenotype closely matches that of *gbpC*$^{-}$/*gbpD*$^{-}$ cells that has been reported (Bosgraaf et al., 2002a). In contrast to *gbpC*$^{-}$ cells, *gbpD*$^{-}$ cells displayed enhanced chemotaxis caused by a reduced tendency to make lateral pseudopodia and a higher speed. The latter is presumably caused by the reduced substrate adhesion that was observed. Cells overexpressing GbpD protein were very flattened and produced an unusual amount of lateral pseudopodia that often bifurcated. These cells attached more strongly to the substrate, which led to a decreased cell speed. Moreover, cells were no longer capable of aggregation, and chemotaxis was severely impaired owing to a lack of directionality and polarity. These findings indicate that GbpC is needed for polarity and efficient chemotaxis, whereas GbpD induces the formation of substrate attached pseudopodia, thereby negatively influencing cell speed and polarity.

Although the chemotaxis index of *gbpC*$^{-}$ cells was close to zero, this mutant is still capable of aggregation on agar in a relatively normal way. One possible explanation is that when plated at high density, cells probably need little chemotaxis in order to form aggregates. Another reason could be that *gbpC*$^{-}$ cells display better chemotaxis when placed on a different surface; we observed that *gbpC*$^{-}$ cells have improved, but still aberrant chemotaxis when placed on a glass surface instead of the Perspex surface that was used for the experiments described in this paper. The chemotaxis index increased to about 0.3 in this case (L.B. and P.J.M.v.H., unpublished). In contrast to this, GbpD overexpressing cells behaved identical on glass and Perspex surfaces, displaying highly impaired chemotaxis (L.B. and P.J.M.v.H., unpublished). In accordance with this observation, this mutant was unable to aggregate or form fruiting bodies.

### Cell-surface attachment

The faster cell movement that was observed in starved *gbpD*$^{-}$ cells was presumably caused by a weaker adhesion to the substratum. Moreover, overexpression of GbpD protein caused a dramatic increase in the adhesion strength to the substratum and a concurrent decrease in cell speed. Recently it was shown that actin foci are located close to the substratum and transmit traction force to the substratum, indicating that these are the sites of cell substrate anchoring (Uchida and Yumura, 2004). We therefore expected that overexpression of GbpD protein would lead to a higher number of actin foci. We found that although the amount of actin foci is higher in cells overexpressing GbpD protein, it is not significantly different from the values of the parent strain. This could be due to the large spread that was found in the amount of foci per cell. However, if the number of foci per cell is divided by the contact area (which might be a more correct measure), the values are virtually identical in *gbpD*$^{-}$/GbpD$^{OE}$ and *gbpD*$^{-}$ cells (0.61 and 0.62 respectively). We propose that the significantly increased number of surface attached protrusions in *gbpD*$^{-}$/GbpD$^{OE}$ cells causes the enhanced surface adhesion and flattening of the cells.

### Myosin-GFP translocation

We found that in *gbpC*$^{-}$ cells, cAMP-induced myosin-GFP translocation to the cortex was lost, whereas *gbpD*$^{-}$ mutants displayed no aberrancies. It is noteworthy that in *gbpC*$^{-}$ cells

moving in buffer, myosin-GFP was still localised in the posterior half of the cell (data not shown). Therefore, there must be a GbpC-independent mechanism that mediates myosin II translocation to the posterior half of unstimulated cells, although cAMP-induced myosin translocation is dependent on GbpC.

The use of GFP-labelled myosin was recently used to study cAMP-regulated myosin behaviour (Levi et al., 2002). In that study, the myosin-GFP translocation was not preceded by a depletion from the membrane and was stronger and more prolonged. These differences are possibly caused by the distinct treatment of the cells; in our study, cells were starved on solid support under phosphate buffer until the ripple stage was reached, whereas Levi and co-workers applied periodic cAMP pulses to cells that were kept in suspension by shaking (Levi et al., 2002).

As in *gbpC*$^{-}$/*gbpD*$^{-}$ cells (Bosgraaf et al., 2002a), cAMP-induced MHC phosphorylation was slightly decreased in *gbpC* single knockout cells (L.B., P.J.M.v.H. and J. Smith, unpublished). As diminished heavy chain phosphorylation should lead to increased filament formation, this cannot account for the observed decrease in cAMP-induced MHC translocation in *gbpC*$^{-}$ cells. Myosin II translocation is also known to be dependent on the presence of filamentous actin (Levi et al., 2002), therefore GbpC could mediate the cAMP-induced binding of myosin to F-actin.

There are at least two other proteins that also participate in myosin II translocation to the cortex. One is RegA (Wessels et al., 2000), a cAMP-selective phosphodiesterase that also serves as a response regulator (Thomason et al., 1999). The other is PAKa, a serine/threonine protein kinase that colocalises with myosin II in migrating cells (Chung and Firtel, 1999; Muller-Taubenberger et al., 2002). As the mechanisms by which these proteins influence myosin II translocation are currently unknown, it remains to be determined whether they interact with GbpC.

## cAMP-induced actin response

As *gbpD*$^{-}$/GbpD$^{OE}$ cells produce many lamellipodia and pseudopodia, we expected a higher level of filamentous actin in unstimulated cells. However, this was not observed. A possible explanation is that the cells were kept in suspension during the actin polymerisation assay. The cells probably become less flattened and possibly lose their pseudopodia under these circumstances. Furthermore, F-actin was enriched primarily at the surface contact area in cells overexpressing GbpD protein. At 2 μm above the surface, F-actin distribution appeared normal. As suspended cells do not experience any surface, cells overexpressing GbpD protein could behave relatively normally when kept in suspension. The cAMP-induced actin polymerisation of *gbpD* overexpressing cells was altered compared to wild-type cells; recovery to basal levels was significantly delayed. This indicates that GbpD acts on a signal transduction pathway that influences actin polymerisation.

## cAMP and cGMP binding of GbpD

Although GbpD contains two cyclic nucleotide binding domains, we could not measure any increase of cAMP or cGMP binding activity in cell lysates of cells overexpressing GbpD protein. The same result was obtained when we overexpressed the GFP protein fused to the C-terminal half of GbpD, containing only the cyclic nucleotide binding domains and the GRAM domain. Lysates of cells overexpressing the corresponding C-terminal part of GbpC fused to GFP retained their cGMP binding capacity. Furthermore, the fluorescent signal observed in ΔNGbpC-GFP and ΔNGbpD-GFP expressing cells was comparable, indicating that the protein expression levels were approximately the same. The cGMP-binding capacity of this GbpC-overexpressor strain as determined by Scatchard plots is approximately 0.8 pmol/mg protein (data not shown). Assuming the same protein expression level of GbpD, we can calculate the maximal possible dissociation constant for cAMP and cGMP that is still consistent with the data. The s.e.m. represents the maximal binding activity, which is 0.125 pmol/mg for cGMP and 0.045 pmol/mg for cAMP (ΔN-GbpD-GFP expressing cells; error bars in Fig. 6A). As 50 nM label was used in these experiments, the dissociation constant of GbpD must be higher than 270 nM for cGMP and higher than 840 nM for cAMP. In wild-type cells the concentration of cGMP and cAMP reaches levels up to 2 μM during stimulation, so it cannot be totally excluded that GbpD is regulated by cyclic nucleotides during peak concentrations. However, the striking flattened phenotype and the strong substrate adhesion were not diminished when GbpD was overexpressed in cell lines that have undetectable cAMP and/or cGMP concentrations (see Materials and Methods section). This indicates that GbpD can act without cyclic nucleotides, and we conclude that GbpD is not strongly regulated by intracellular cAMP or cGMP. In this respect, it is noteworthy that a family of proteins has been identified in mammalian cells that also contain RasGEF and cyclic nucleotide domains (Kuiperij et al., 2003). Two of these, Epac1 and Epac-2, bind cAMP with physiological affinity and specifically activate Rap in a cAMP-dependent manner (de Rooij et al., 1998; Rehmann et al., 2003). However, two other proteins of this family, PDZ-GEF 1 and 2, display guanine nucleotide exchange activity but are not activated by cAMP or 8Br-cGMP (Kuiperij et al., 2003). Furthermore, the purified cyclic nucleotide binding domains of PDZ-GEF 1 do not bind cAMP, cGMP or a number of other small molecules (de Rooij et al., 1999; Kuiperij et al., 2003). Thus, like GbpD, the PDZ-GEFs also seem to function without cyclic nucleotides. Remarkably, these proteins specifically activate Rap1, which is an important regulator of integrin-mediated cell adhesion (Bos et al., 2003). We have shown in this article that GbpD also influences cell adhesion. Moreover, as overexpression of the *Dictyostelium* Rap1 homologue induces the same flattened cell morphology as GbpD overexpression (Rebstein et al., 1993), Rap1 may well be a target of GbpD.

In summary, we conclude that GbpC and GbpD have differential functions in *Dictyostelium* chemotaxis and probably act via different signal transduction pathways; GbpC is regulated by cGMP and is needed for chemoattractant-induced myosin translocation and cell polarisation. On the other hand, GbpD does not depend on intracellular cyclic nucleotides and induces surface attached lateral pseudopodia, which provokes depolarisation and enhanced substrate adhesion leading to reduced cell motility. Thus, these two proteins independently affect chemotactic motility in opposing

manners. The exact temporal and spatial regulation of GbpC and GbpD proteins might play an important role in the chemotactic movement of *Dictyostelium* cells.

We thank Janet Smith for stimulating discussions on the *gbpC* knockout data. We thank Thomas Egelhoff and Jeffrey Williams for providing the plasmids encoding myosin-GFP and hygromycin resistant gene, respectively.

## References

**Berlot, C. H., Spudich, J. A. and Devreotes, P. N.** (1985). Chemoattractant-elicited increases in myosin phosphorylation in Dictyostelium. *Cell* **43**, 307-314.

**Bos, J. L., de Bruyn, K., Enserink, J., Kuiperij, B., Rangarajan, S., Rehmann, H., Riedl, J., de Rooij, J., van Mansfeld, F. and Zwartkruis, F.** (2003). The role of Rap1 in integrin-mediated cell adhesion. *Biochem. Soc. Trans.* **31**, 83-86.

**Bosgraaf, L., Russcher, H., Smith, J. L., Wessels, D., Soll, D. R. and van Haastert, P. J.** (2002a). A novel cGMP signalling pathway mediating myosin phosphorylation and chemotaxis in Dictyostelium. *EMBO J.* **21**, 4560-4570.

**Bosgraaf, L., Russcher, H., Snippe, H., Bader, S., Wind, J. and van Haastert, P. J. M.** (2002b). Identification and characterization of two unusual cGMP-stimulated phoshodiesterases in Dictyostelium. *Mol. Biol. Cell.* **13**, 3878-3889.

**Chung, C. Y. and Firtel, R. A.** (1999). PAKa, a putative PAK family member, is required for cytokinesis and the regulation of the cytoskeleton in Dictyostelium discoideum cells during chemotaxis. *J. Cell Biol.* **147**, 559-576.

**Clow, P. A. and McNally, J. G.** (1999). In vivo observations of myosin II dynamics support a role in rear retraction. *Mol. Cell. Biol.* **10**, 1309-1323.

**Condeelis, J., Hall, A., Bresnick, A., Warren, V., Hock, R., Bennett, H. and Ogihara, S.** (1988). Actin polymerization and pseudopod extension during amoeboid chemotaxis. *Cell Motil. Cytoskeleton* **10**, 77-90.

**de Rooij, J., Zwartkruis, F. J., Verheijen, M. H., Cool, R. H., Nijman, S. M., Wittinghofer, A. and Bos, J. L.** (1998). Epac is a Rap1 guanine-nucleotide-exchange factor directly activated by cyclic AMP. *Nature* **396**, 474-477.

**de Rooij, J., Boenink, N. M., van Triest, M., Cool, R. H., Wittinghofer, A. and Bos, J. L.** (1999). PDZ-GEF1, a guanine nucleotide exchange factor specific for Rap1 and Rap2. *J. Biol. Chem.* **274**, 38125-38130.

**Dormann, D., Libotte, T., Weijer, C. J. and Bretschneider, T.** (2002). Simultaneous quantification of cell motility and protein-membrane-association using active contours. *Cell Motil. Cytoskeleton* **52**, 221-230.

**Egelhoff, T. T., Lee, R. J. and Spudich, J. A.** (1993). Dictyostelium myosin heavy chain phosphorylation sites regulate myosin filament assembly and localization in vivo. *Cell* **75**, 363-371.

**Egelhoff, T. T., Naismith, T. V. and Brozovich, F. V.** (1996). Myosin-based cortical tension in Dictyostelium resolved into heavy and light chain-regulated components. *J. Muscle Res. Cell Motil.* **17**, 269-274.

**Fey, P., Stephens, S., Titus, M. A. and Chisholm, R. L.** (2002). SadA, a novel adhesion receptor in Dictyostelium. *J. Cell Biol.* **159**, 1109-1119.

**Goldberg, J. M., Bosgraaf, L., van Haastert, P. J. M. and Smith, J. L.** (2002). Identification of four candidate cGMP targets in Dictyostelium. *Proc. Natl. Acad. Sci. USA* **99**, 6749-6754.

**Griffith, L. M., Downs, S. M. and Spudich, J. A.** (1987). Myosin light chain kinase and myosin light chain phosphatase from Dictyostelium: effects of reversible phosphorylation on myosin structure and function. *J. Cell Biol.* **104**, 1309-1323.

**Heid, P. J., Wessels, D., Daniels, K. J., Gibson, D. P., Zhang, H., Voss, E. and Soll, D. R.** (2004). The role of myosin heavy chain phosphorylation in Dictyostelium motility, chemotaxis and F-actin localization. *J. Cell Sci.* **117**, 4819-4835.

**Khurana, B., Khurana, T., Khaire, N. and Noegel, A. A.** (2002). Functions of LIM proteins in cell polarity and chemotactic motility. *EMBO J.* **21**, 5331-5342.

**Koehl, G. and McNally, J. G.** (2002). Myosin II redistribution during rear retraction and the role of filament assembly and disassembly. *Cell Biol. Int.* **26**, 287-296.

**Kuiperij, H. B., de Rooij, J., Rehmann, H., van Triest, M., Wittinghofer, A., Bos, J. L. and Zwartkruis, F. J.** (2003). Characterisation of PDZ-GEFs, a family of guanine nucleotide exchange factors specific for Rap1 and Rap2. *Biochim. Biophys. Acta.* **1593**, 141-149.

**Laevsky, G. and Knecht, D. A.** (2003). Cross-linking of actin filaments by myosin II is a major contributor to cortical integrity and cell motility in restrictive environments. *J. Cell Sci.* **116**, 3761-3770.

**Lee, E., Pang, K. and Knecht, D.** (2001). The regulation of actin polymerization and cross-linking in Dictyostelium. *Biochim. Biophys. Acta*. **1525**, 217-227.

**Levi, S., Polyakov, M. V. and Egelhoff, T. T.** (2002). Myosin II dynamics in Dictyostelium: determinants for filament assembly and translocation to the cell cortex during chemoattractant responses. *Cell Motil. Cytoskeleton* **53**, 177-188.

**Linskens, M. H., Grootenhuis, P. D., Blaauw, M., Huisman-de Winkel, B., van Ravestein, A., van Haastert, P. J. and Heikoop, J. C.** (1999). Random mutagenesis and screening of complex glycoproteins: expression of human gonadotropins in Dictyostelium discoideum. *FASEB J.* **13**, 639-345.

**Liu, G. and Newell, P. C.** (1991). Evidence of cyclic GMP may regulate the association of myosin II heavy chain with the cytoskeleton by inhibiting its phosphorylation. *J. Cell Sci.* **98**, 483-490.

**Meima, M. E., Biondi, R. M. and Schaap, P.** (2002). Identification of a novel type of cGMP phosphodiesterase that is defective in the chemotactic stmF mutants. *Mol. Biol. Cell* **13**, 3870-3877.

**Moores, S. L., Sabry, J. H. and Spudich, J. A.** (1996). Myosin dynamics in live Dictyostelium cells. *Proc. Natl. Acad. Sci. USA* **93**, 443-446.

**Muller-Taubenberger, A., Bretschneider, T., Faix, J., Konzok, A., Simmeth, E. and Weber, I.** (2002). Differential localization of the Dictyostelium kinase DPAKa during cytokinesis and cell migration. *J. Muscle Res. Cell Motil.* **23**, 751-763.

**Mutzel, R., Simon, M. N., Lacombe, M. L. and Veron, M.** (1988). Expression and properties of the regulatory subunit of Dictyostelium cAMP-dependent protein kinase encoded by lambda gt11 cDNA clones. *Biochemistry* **27**, 481-486.

**Potma, E., de Boeij, W. P., van Haastert, P. J. and Wiersma, D. A.** (2001). Real-time visualization of intracellular hydrodynamics in single living cells. *Proc. Natl. Acad. Sci. USA* **98**, 1577-1582.

**Rebstein, P. J., Weeks, G. and Spiegelman, G. B.** (1993). Altered morphology of vegetative amoebae induced by increased expression of the Dictyostelium discoideum ras-related gene rap1. *Dev. Genet.* **14**, 347-355.

**Rehmann, H., Prakash, B., Wolf, E., Rueppel, A., de Rooij, J., Bos, J. L. and Wittinghofer, A.** (2003). Structure and regulation of the cAMP-binding domains of Epac2. *Nat. Struct. Biol.* **10**, 26-32.

**Roelofs, J. and van Haastert, P. J.** (2002). Characterization of two unusual guanylyl cyclases from dictyostelium. *J. Biol. Chem.* **277**, 9167-9174.

**Roelofs, J., Meima, M., Schaap, P. and van Haastert, P. J. M.** (2001a). The Dictyostelium. homologue of mammalian soluble adenylyl cyclase encodes a guanylyl cyclase. *EMBO J.* **20**, 4341-4348.

**Roelofs, J., Snippe, H., Kleineidam, R. G. and van Haastert, P. J. M.** (2001b). Guanylate cyclase in Dictyostelium discoideum with the topology of mammalian adenylate cyclase. *Biochem. J.* **354**, 697-706.

**Schneider, N., Weber, I., Faix, J., Prassler, J., Muller-Taubenberger, A., Kohler, J., Burghardt, E., Gerisch, G. and Marriott, G.** (2003). A Lim protein involved in the progression of cytokinesis and regulation of the mitotic spindle. *Cell Motil. Cytoskeleton* **56**, 130-139.

**Soll, D. R.** (1995). The use of computers in understanding how animal cells crawl. *Int. Rev. Cytol.* **163**, 43-104.

**Soll, D. R., Wessels, D., Voss, E. and Johnson, O.** (2001). Computer-assisted systems for the analysis of amoeboid cell motility. *Methods Mol. Biol.* **161**, 45-58.

**Stites, J., Wessels, D., Uhl, A., Egelhoff, T., Shutt, D. and Soll, D. R.** (1998). Phosphorylation of the Dictyostelium myosin II heavy chain is necessary for maintaining cellular polarity and suppressing turning during chemotaxis. *Cell Motil. Cytoskeleton* **39**, 31-51.

**Thomason, P. A., Traynor, D., Stock, J. B. and Kay, R. R.** (1999). The RdeA-RegA system, a eukaryotic phospho-relay controlling cAMP breakdown. *J. Biol. Chem.* **274**, 27379-27384.

**Uchida, K. S. and Yumura, S.** (2004). Dynamics of novel feet of Dictyostelium cells during migration. *J. Cell Sci.* **117**, 1443-1455.

**van Haastert, P. J. and Kuwayama, H.** (1997). cGMP as second messenger during Dictyostelium chemotaxis. *FEBS Lett*. **410**, 25-28.

**Varnum, B. and Soll, D. R.** (1984). Effects of cAMP on single cell motility in Dictyostelium. *J. Cell Biol.* **99**, 1151-1155.

**Wessels, D., Soll, D. R., Knecht, D., Loomis, W. F., de Lozanne, A. and**

**Spudich, J.** (1988). Cell motility and chemotaxis in Dictyostelium amebae lacking myosin heavy chain. *Dev. Biol.* **128**, 164-177.

**Wessels, D. J., Zhang, H., Reynolds, J., Daniels, K., Heid, P., Lu, S., Kuspa, A., Shaulsky, G., Loomis, W. F. and Soll, D. R.** (2000). The internal phosphodiesterase RegA is essential for the suppression of lateral pseudopods during Dictyostelium chemotaxis. *Mol. Biol. Cell* **11**, 2803-2820.

**Zhang, H., Wessels, D., Fey, P., Daniels, K., Chisholm, R. L. and Soll, D. R.** (2002). Phosphorylation of the myosin regulatory light chain plays a role in motility and polarity during Dictyostelium chemotaxis. *J. Cell Sci.* **115**, 1733-1747.

**Zhang, H., Heid, P. J., Wessels, D., Daniels, K. J., Pham, T., Loomis, W. F. and Soll, D. R.** (2003). Constitutively active protein kinase A disrupts motility and chemotaxis in *Dictyostelium discoideum*. *Eukaryot. Cell* **2**, 62-75.

**Zigmond, S. H., Joyce, M., Borleis, J., Bokoch, G. M. and Devreotes, P. N.** (1997). Regulation of actin polymerization in cell-free systems by GTPgammaS and Cdc42. *J. Cell Biol.* **138**, 363-374.